

Time-Reversal UWB Imaging with a Single Antenna in Multi-Path Environments

Takuya Sakamoto ¹, Toru Sato ²

*Department of Communications and Computer Engineering, Graduate School of Informatics, Kyoto University
Yoshida-Honmachi, Sakyo-ku, Kyoto 606-8501, Japan*

¹t-sakamo@i.kyoto-u.ac.jp

²tsato@kuee.kyoto-u.ac.jp

Abstract—Electromagnetic inverse scattering with TR (Time-Reversal) imaging has been studied with great interest in a variety of applications. In this study, we propose a UWB radar system with a single antenna that utilizes multi-path scattering. The proposed imaging method is an extension of the conventional DORT method, and uses a frequency-frequency matrix that is suitable for a system with a single antenna. The performance of the proposed method is investigated by means of a numerical simulation and an experiment.

I. INTRODUCTION

Electromagnetic inverse scattering with TR (Time-Reversal) imaging has been studied with great interest in a variety of applications. Most of the studies involving TR inverse scattering assume that multiple signals are observed at several antenna locations, which naturally implies costly array antennas. In this study, we propose a simple UWB radar system with a single antenna that utilizes multi-path scattering. The proposed imaging method is an extension of the DORT (French acronym for decomposition of the time reversal operator) method, which was developed for systems with array antennas, and is based on a SVD (Singular Value Decomposition) of a matrix. A variety of matrices can be used, such as a space-space matrix[1] or a space-frequency matrix [2]. The method proposed in this study uses a frequency-frequency matrix that is suitable for a system with a single antenna. Some research groups have studied multiple scattering between point-like targets[3], [4], [5], but they have assumed array antennas, which are not applicable to our system. The performance of the proposed method is investigated by means of a numerical simulation and an experiment.

II. SYSTEM MODEL

Fig. 1 shows a model of the system proposed in this study. The problem is imaging on a 2-dimensional plane. Distances are normalized by the center wavelength λ of a transmitted pulse, while propagation is calculated with a Green's function in the imaging process. The Green's function for the numerical simulation is expressed as

$$G(\omega, \mathbf{r}, \mathbf{r}') = -\frac{j}{4} H_0 \left(\frac{\omega}{c} |\mathbf{r} - \mathbf{r}'| \right), \quad (1)$$

where H_0 is a Hankel function of the first kind, and \mathbf{r} and \mathbf{r}' are the positions of the ends of a propagation path. Scattering

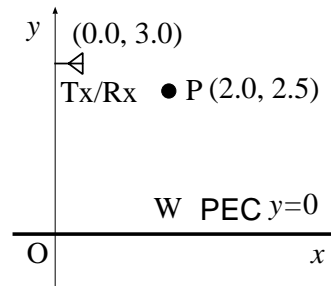


Fig. 1. System model of a multi-path scattering UWB radar.

by a point target is modeled with the Born approximation as

$$S(\omega) = \int \omega^2 \sigma(\mathbf{r}') G^2(\omega, \mathbf{r}, \mathbf{r}') d\mathbf{r}', \quad (2)$$

where $\sigma(\mathbf{r}')$ is the relative permittivity at position \mathbf{r}' . This system is composed of a transmit antenna Tx, a receiving antenna Rx, a plate W made of a PEC (Perfectly Electric Conductor), and a point-like PEC target P. The transmitted pulse is a UWB pulse $s_T(t)$, which is a mono-cycle pulse for the numerical simulation. We assume that the relative locations of the antennas and the plate are known. The direct wave $s_D(t)$ from Tx to Rx without scattering, and the reflected wave $s_W(t)$ from plate W are measured and stored in memory prior to the actual measurement of the targets. Waveforms $s_D(t)$ and $s_W(t)$ are subtracted from a received signal $s_0(t)$ as $s(t) = s_0(t) - s_D(t) - s_W(t)$. We assume that $s(t)$ contains 4 waves, namely

- $s_1(t)$ Tx-P-Rx,
- $s_2'(t)$ Tx-P-W-Rx,
- $s_2''(t)$ Tx-W-P-Rx, and
- $s_3(t)$ Tx-W-P-W-Rx,

where $s_2'(t)$ and $s_2''(t)$ correspond to a pair of paths with opposite directions. Therefore, these echoes cannot be separated if the system satisfies the condition of the Lorentz reciprocal theorem. Hereafter, only 3 paths are considered, by introducing $s_2(t) = s_2'(t) + s_2''(t)$. Additionally, note that this model neglects higher-order multiple scattering components.

III. CONVENTIONAL TIME-REVERSAL IMAGING AND DORT

TR imaging makes use of the Lorentz reciprocal theorem, and is characterized by its simple signal processing. The principle of TR is described below. Let $s(t)$ be the received signal at Rx when a pulse is transmitted from Tx at $t = 0$. Assume that $s(-t)$ is transmitted from Rx, then a strong signal is received at Tx at $t = 0$.

Next, we introduce $G(\omega, \mathbf{r}, \mathbf{r}')$, the Green's function of propagation in the assumed medium, which includes the effect of multi-path scattering. Then $S(\omega)$, the Fourier transform of the received signal $s(t)$, is expressed using $S_T(\omega)$, the Fourier transform of a transmitted signal $s_T(t)$, as

$$S(\omega) = \omega^2 G^2(\omega, \mathbf{r}, \mathbf{r}') S_T(\omega), \quad (3)$$

disregarding constant terms, and where the positions of both Tx and Rx are \mathbf{r} and the position of the point target is \mathbf{r}' . Here, we assume Rayleigh scattering with a tiny scatterer. Note that the time reversal operator is equivalent to a complex conjugate operation. Therefore, the image from TR method $I_{TR}(\mathbf{x})$ is obtained as

$$\begin{aligned} I_{TR}(\mathbf{x}) &= \int S^* S_T(\omega) (\omega) G^2(\omega, \mathbf{r}, \mathbf{x}) d\omega, \\ &= \int \omega^2 |S_T(\omega)|^2 G^{*2}(\omega, \mathbf{r}, \mathbf{r}') G^2(\omega, \mathbf{r}, \mathbf{x}) d\omega \end{aligned} \quad (4)$$

The value of $I_{TR}(\mathbf{x})$ in Eq. (5) is at its maximum when $\mathbf{x} = \mathbf{r}'$ because the integrand is a real function. As mentioned above, this classical TR method is based on matched filter theory.

DORT is an extension of TR imaging that introduces SVD to improve the resolution. With a space-space matrix K_{SS} , DORT assumes that a sinusoidal wave is transmitted, and there are multiple transmitting and receiving antennas. Element $k_{i,j}$ of K_{SS} is defined as the received complex signal between the i -th transmitting antenna and the j -th receiving antenna. Here, $k_{i,j}$ is expressed as

$$k_{i,j} = \sum_{l=1}^K \sigma_l g_{i,l} g_{l,j}, \quad (6)$$

where $g_{i,l}$ is the Green's function between the i -th antenna and the l -th target, and σ_l is in proportion to the scattering intersection of the l -th target. The three terms in Eq. (6) can be divided into three elements of matrices as

$$K_{SS} = U \Sigma V^H, \quad (7)$$

where U and V are composed of $g_{i,l}$ and $g_{l,j}$, respectively. Here, Σ is a diagonal matrix consisting of with σ_l . The Green's function for each propagation path is divided into two matrices U and V , thus enabling an imaging just like the classical MUSIC method because we can derive a noise subspace by checking the elements of Σ . This procedure is illustrated in Fig. 2. Although this method works well in the assumed model with a sinusoidal wave and multiple antennas, it cannot be applied to our system without an appropriate extension.

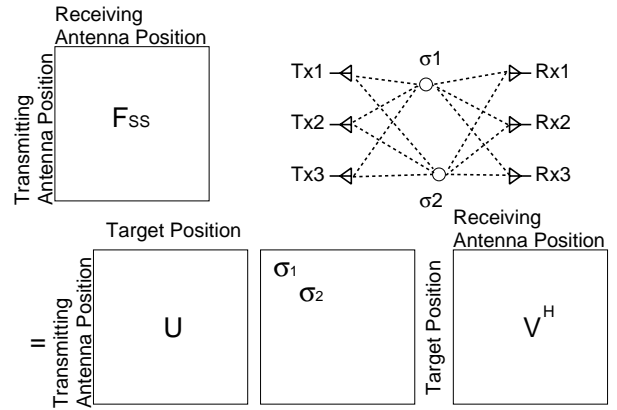


Fig. 2. Singular value decomposition of a space-space matrix in the conventional DORT.

IV. PROPOSED COARSE-FINE-FREQUENCIES DORT

S_1, \dots, S_N is defined as the value of the received signal $S(\omega)$ in the frequency domain at $\omega_1, \dots, \omega_N$. The matrix K_{FF} is defined as

$$K_{FF} = \begin{bmatrix} S_1 & S_2 & \cdots & S_L \\ S_{L+1} & S_{L+2} & \cdots & S_{2L} \\ \vdots & \vdots & \vdots & \vdots \\ S_{N-L+1} & S_{N-L+2} & \cdots & S_N \end{bmatrix}, \quad (8)$$

where the rows and columns correspond to coarse and fine changes in frequencies, respectively. We assume $N = L^2$ for simplicity. For comparison with the conventional DORT, Fig. 3 shows the SVD of the K_{FF} . In the proposed method, the Green's function is expressed as

$$G(\omega + \Delta\omega, \mathbf{r}', \mathbf{r}) \simeq -\frac{j}{4} \frac{\exp\left(j \frac{\omega + \Delta\omega}{c} |\mathbf{r} - \mathbf{r}'|\right)}{\sqrt{\frac{\omega + \Delta\omega}{c} |\mathbf{r} - \mathbf{r}'|}} \quad (9)$$

$$\simeq -\frac{j}{4} \frac{\exp\left(j \frac{\omega}{c} |\mathbf{r} - \mathbf{r}'|\right)}{\sqrt{\frac{\omega}{c} |\mathbf{r} - \mathbf{r}'|}} \quad (10)$$

$$\cdot \exp\left(j \frac{\Delta\omega}{c} |\mathbf{r} - \mathbf{r}'|\right), \quad (11)$$

where ω and $\Delta\omega$ are coarse and fine frequencies, respectively. With this approximation, the Green's function for each propagation path can be divided into two parts, which forms the basis of our proposed method.

First, the proposed DORT applies SVD to K_{FF} as

$$K_{FF} = U \Sigma V^H, \quad (12)$$

where Σ is a diagonal matrix with singular values. The left and right singular matrices correspond to coarse and fine frequencies, respectively. As in the conventional DORT, we adopt small $L - PK$ singular values to estimate noise subspaces, where P is the number of multipaths for each point-like target, and K is the number of targets. In this paper we assume $P = 3$ and $K = 1$. We select left and right singular vectors, $\mathbf{u}_{PK+1} \cdots \mathbf{u}_N$ and $\mathbf{v}_{PK+1} \cdots \mathbf{v}_N$, respectively, as the

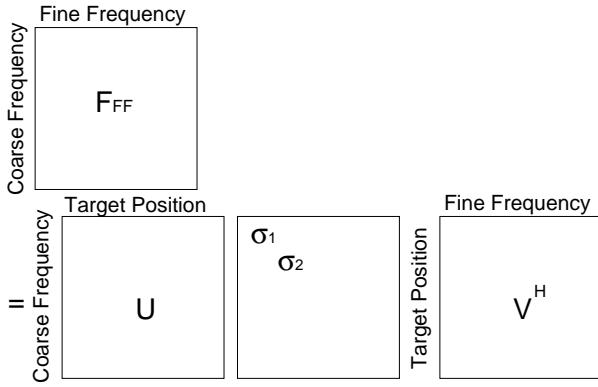


Fig. 3. Singular value decomposition of a space-space matrix in the proposed DORT.

base vectors of the noise subspace and obtain the image from the left singular vectors as

$$I_L(\mathbf{x}) = \frac{1}{\sum_{i=PK+1}^L \sum_{p=1}^P |\mathbf{u}_i^H \mathbf{g}_p(\mathbf{x})|^2 / |\mathbf{g}_p(\mathbf{x})|^2}, \quad (13)$$

where \mathbf{g}_p is the L -dimensional vector with values of the Green's function for the p -th path at $\omega_1, \omega_{L+1}, \dots, \omega_{N-L+1}$. Similarly, the image $I_R(\mathbf{x})$ can be obtained from the right singular vectors. We obtain the final image by multiplying these as $I_{DORT}(\mathbf{x}) = I_L(\mathbf{x})I_R(\mathbf{x})$.

V. PERFORMANCE EVALUATION OF IMAGING METHODS

Examples of applying the conventional and proposed methods are given in this section. As in shown in Fig. 1, the PEC plate is on the x -axis, the antenna is on the y -axis, and the target is at $(2.0\lambda, 2.5\lambda)$. The propagation model is approximated as a scalar wave with the Green's function described above, and we assume a noiseless case for the numerical simulation. In the proposed method, we set $L = 10$ and $N = 100$ while $L - PK = 7$ small singular values are selected from the 10×10 matrix K_{FF} , and the corresponding 7 left and right singular vectors are used for imaging.

The signal used in this numerical simulation is shown in Fig. 4, where the solid line represents the transmitted pulse and the dashed line the received echoes. There are three echoes from three different paths in this figure. The time-reversal image I_{TR} is shown in Figs. 5 and 6, where cross symbols denote the actual target positions. This image I_{TR} has the maximum value at the actual location, but there are many undesired false peaks, that causes the poor image resolution.

The image from the left singular matrix $I_L(\mathbf{x})$ is shown in Fig. 7. Although the actual target position is estimated with a high resolution, there are other undesired peaks in the figure. The image from the right singular matrix $I_R(\mathbf{x})$ is shown in Fig. 8. Although there are no undesired false images, the resolution is lower than that of $I_L(\mathbf{x})$. The proposed method obtains the final image by multiplying these images as $I_{DORT}(\mathbf{x}) = I_L(\mathbf{x})I_R(\mathbf{x})$. The proposed DORT image

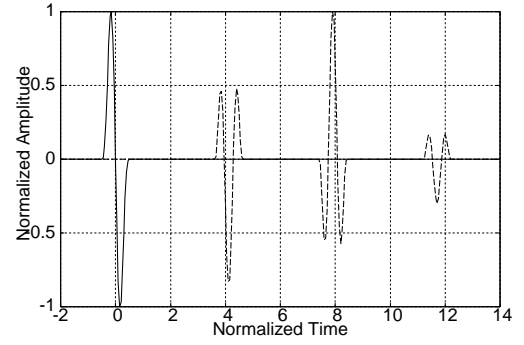


Fig. 4. Received signal used in the numerical simulation.

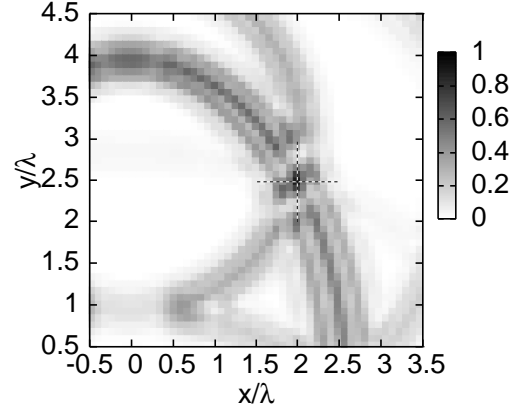


Fig. 5. Conventional time-reversal image with numerical data.

I_{DORT} is shown in Figs. 9 and 10 and this image has a higher resolution than the conventional one.

Next, we apply the imaging methods to experimental data. Fig. 11 shows the experimental UWB radar site in an anechoic chamber. The system includes a short pulse generator, a pair of omni-directional wideband planar patch antennas, and a wideband oscilloscope. The transmitted pulse has a center frequency of 3.7GHz and bandwidth of 3.0GHz. A metallic pole with a diameter of 5mm is used instead of the point-like target assumed in the numerical simulation described above. This pole is set parallel to the baseline of the pair of antennas. The differences between this experiment and the numerical simulation are

- the target used is not a point target in the strictest sense,
- a 3-dimensional Green's function should be employed instead of the 2-dimensional one,
- the bandwidth is limited by the antenna property, and
- different antennas are used for transmitting and receiving.

All these differences, except the first one regarding the size of the target, are taken into account in the imaging signal processing. Fig. 12 shows a transmitted and a received signal in this experiment. After subtracting the direct wave from the metallic plate W from the received signal, we obtain the echoes caused by the multi-path scattering as shown in Fig. 13. The three echoes are clearly observed in this figure, highlighted by

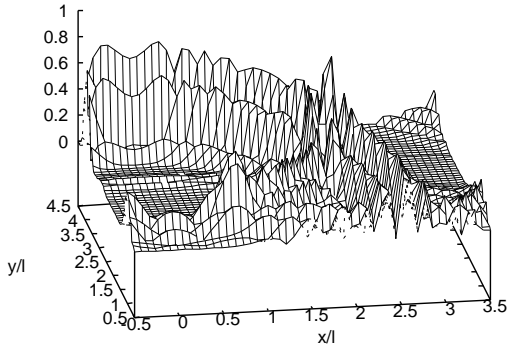


Fig. 6. Conventional time-reversal 3-D image with numerical data.

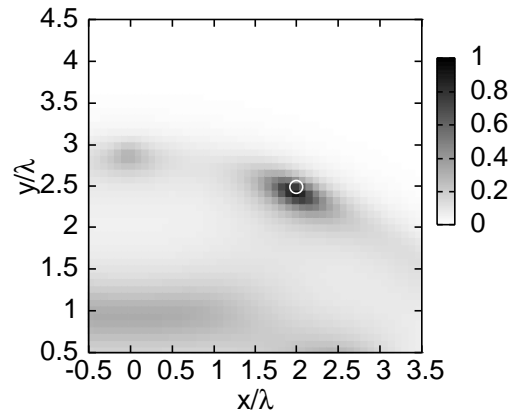


Fig. 8. DORT image with a fine frequency noise subspace.

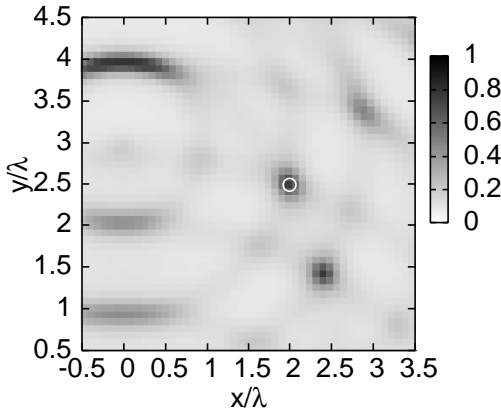


Fig. 7. DORT image with a coarse frequency noise subspace.

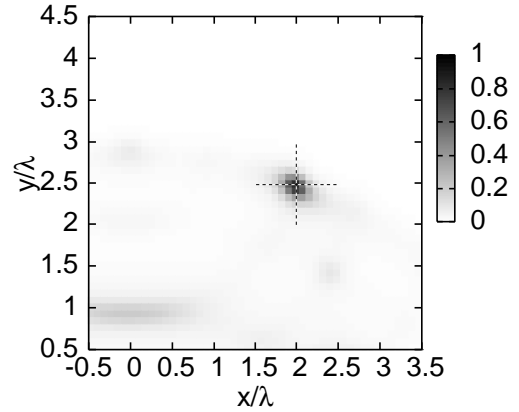


Fig. 9. Proposed DORT image with numerical data.

black triangles.

Figs. 14 and 15 show the images obtained from the conventional time-reversal method and the proposed DORT, respectively. Although the resolution is not as high as that in the numerical simulation because of the effect of noise and timing jitter, the proposed method clearly shows an improvement in the resolution.

VI. CONCLUSION

A new method has been proposed for electromagnetic inverse scattering with time-reversal imaging. This method is applicable to a wide-band radar system with a single antenna. The proposed method has been derived by introducing a frequency-frequency matrix to the conventional DORT, allowing the method to be applied to measurement with a single antenna, whereas the conventional DORT assumes a system with multiple antennas or sinusoidal signals. The performance of the proposed method has been investigated with a numerical simulation and an experiment. Results of both the numerical and experimental investigations show that the proposed method has higher resolution than the conventional time-reversal method.

REFERENCES

- [1] A. J. Devaney, "Time reversal imaging of obscured targets from multistatic data," *IEEE Trans. Antennas and Propagat.*, vol. 53, no. 5, May 2005.
- [2] M. E. Yavuz and F. L. Teixeira, "Space-frequency ultrawideband time-reversal imaging," *IEEE Trans. Geoscience and Remote Sensing*, vol. 46, no. 4, Apr. 2008.
- [3] F. K. Gruber, E. A. Marengo and A. J. Devaney, "Time-reversal imaging with multiple signal classification considering multiple scattering between the targets," *J. Acoust. Soc. Am.*, vol. 115, no. 6, June 2004.
- [4] F. Simonetti, M. Fleming, and E. A. Marengo, "Illustration of the role of multiple scattering in subwavelength imaging from far-field measurements," *J. Opt. Soc. Am.*, vol. 25, no. 2, Feb. 2008.
- [5] R. Solimene, A. Brancaccio, J. Romano, and R. Pierri, "Localizing thin metallic cylinders by a 2.5-D linear distributional approach: experimental results," *IEEE Trans. Antenna Propagation*, vol. 56, no. 8, Aug. 2008.

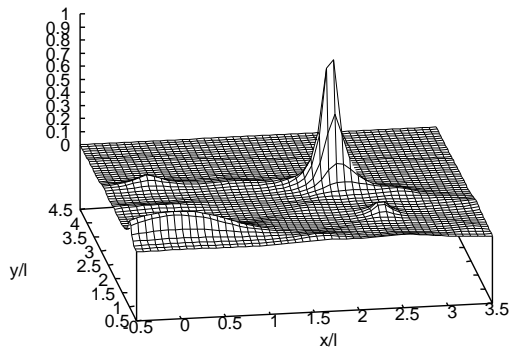


Fig. 10. Proposed DORT 3-D image with numerical data.

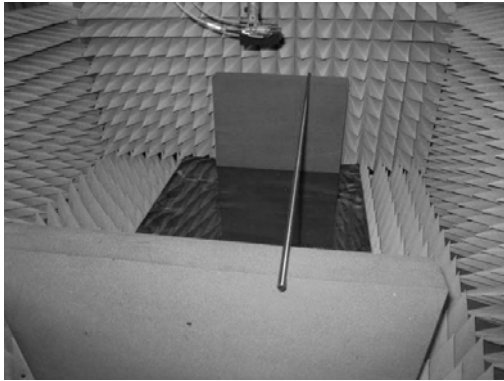


Fig. 11. Experimental setup for UWB radar imaging.

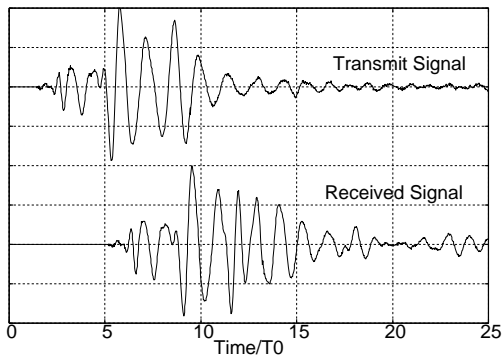


Fig. 12. Transmitted and received signals in the experiment.

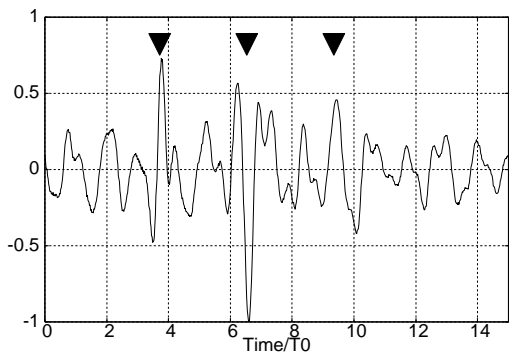


Fig. 13. Received echoes caused by multi-path scattering in the experiment.

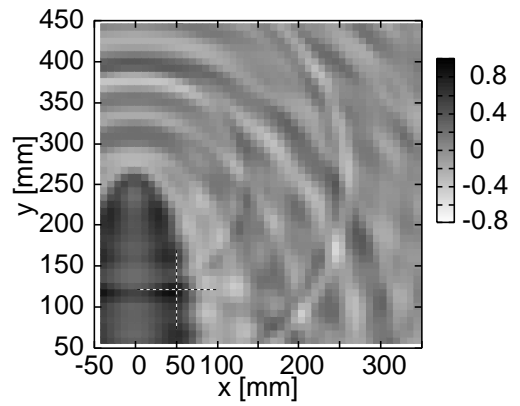


Fig. 14. Conventional time-reversal image with experimental data.

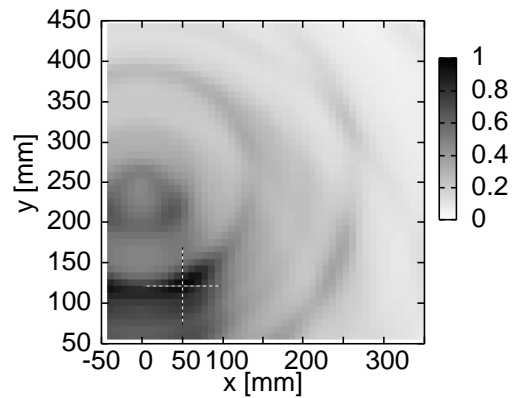


Fig. 15. Proposed DORT image with experimental data.